Fractal-like Triplet Excitation Kinetics and Chromophore Morphology in Blends of Poly(1-vinylnaphthalene) and Poly(methyl methacrylate)

Ching Shan Li and Raoul Kopelman*

Department of Chemistry, The University of Michigan, Ann Arbor, Michigan 48109.
Received October 17, 1988; Revised Manuscript Received June 14, 1989

ABSTRACT: The triplet–triplet annihilation of poly(1-vinylnaphthalene) in poly(methyl methacrylate) (P1VN/PMMA) blends at 77 K is found to be extremely sensitive to the local chromophore morphology. At medium low P1VN concentration, the exciton fusion kinetics is fractal-like, indicative of a quasi-one-dimensional excitation transport topology at about 10%. The dilute-sample phosphorescence decays are very well described by modified stretched exponentials whose exponents also account for the delayed fluorescence decays. This is modeled by pseudomonomolecular kinetics, based on the fusion of free triplet excitations with trapped triplet excitations (excimers). The very dilute P1VN samples may exhibit a crossover from diffusion-limited (fractal-like) to reaction-limited (classical) exciton kinetics. Compared to singlet excitation studies, triplet kinetics provide information on a finer geometrical scale and over a much wider blend concentration range. For the dilute blends, the chromophore triplet excitation topology is quasi-linear, implying a P1VN chain morphology with no significant aggregation or compact globule formation at the limit of very dilute blends.

I. Introduction

The study of electronic excitation transport in solid-state polymer systems can lead to the understanding of the local morphology and the microscopic interactions of the polymer with itself and with its environment. Considerable effort has been devoted to studying energy transport in aromatic polymer blends and copolymers, especially in those with naphthalene pendent groups.[1-14]

Fox and co-workers[1] investigated the singlet excimer formation of aromatic polymers in solid films as well as in solution, and concluded that (i) excimer formation in polystyrene (PS), P1VN, and P2VN is largely intramolecular, but interchain excimers are also formed in the undiluted solid polymers, and (ii) intramolecular excimer sites are highly efficient in trapping excitation but appear not to present a barrier for energy transfer to a deep trap within the polymer chain. Frank and co-workers used the ratio of singlet excimer to singlet excited monomer fluorescence intensity for studying phase separation[2] and compatibility[3] in aromatic polymer blends. Morawetz[4] studied the polymer compatibility by nonradiative singlet energy transfer between two polymeric species labeled with donor and acceptor chromophores, respectively. Fayer and co-workers[5] applied time-resolved fluorescence depolarization techniques to quantitatively evaluate the average root-mean-square radius of gyration in aromatic homopolymer and random copolymer blends.

The delayed emission, due to triplet–triplet annihilation, of solid P2VN[6] and other polymers in glasses[7] at 77 K has been found to increase with molecular weight. Studies of the antenna effect in copolymers of 2-vinylnaphthalene with phenyl vinyl ketone in a rigid glass at 77 K reveal that the naphthalene singlet state is quenched by singlet energy migration and transfer to the aromatic ketone, but the ketone triplet states are in turn quenched by triplet energy transfer to naphthalene, resulting in the offset of the disruption of energy migration due to the separation of naphthalene monomer sequences by the ketone monomer.[8]

Nonexponential molecular relaxation of aromatic polymers in both fluid solutions and solid blends has been studied by applying time-resolved fluorescence techniques.[9] It has been found that the monomer emission can be empirically fit to a weighted sum of three exponentials in P1VN/MMA,[10] P1VN, P2VN, and P1VN/MA[11] in fluid solutions. On the other hand, Frank and co-workers used simple one-dimensional[12] and three-dimensional[13] random walk models to account for the photostationary-state singlet excimer to monomer quantum yield ratios in solutions and solid blends of aromatic vinyl polymers. Furthermore, it was demonstrated[14] that a particular set of numerically fit exponentials cannot uniquely determine the excited-state kinetics in fluorescent polymeric systems. In addition, to account for low dimensionality, disorder, and inhomogeneity in the system of vinyl homopolymer in dilute fluid solution, a trapping function of the form $K(t) = b + ct^{-1/2}$, where b represents the asymptotic discrete hopping rate and c is a hopping frequency, was applied to the transient kinetics of singlet energy migration.[15]

Recently, the application of a "fractal" formalism to interpret the reaction dynamics on random heterogeneous systems such as molecular alloys,[16] glasses,[17] and polymers[18] has been of considerable interest. The anomalous triplet–triplet annihilation kinetics observed in naphthalene when doped in PMMA,[19] sublimed into porous media,[20] and mixed with perdeuterionaphthalene[21] can be well explained by such a fractal approach. However, it has also been shown[20] that fractal-like characteristics may just describe a crossover from one- to three-dimensional topology.

The fractional exponential relaxation (KWW or stretched exponential) function, first introduced by Kohlrausch[22] and in recent times by Williams and Watts[23] in connection with dielectric relaxation, turns out to be a pragmatic empirical model for many relaxation phenomena in glasses and polymers. In addition, applications to electrical, thermal, optical, magnetic, and mechanical phenomena have also been made.[24]

Klafter and Shlesinger[25] have shown the mathematical relationship between three quite different physical models that lead to KWW. What is then the real model for the KWW relaxation function? Can the KWW model be used to explain the anomalous triplet–triplet annihi-

0024-9297/90/2223-2223$02.50/0

lation kinetics? Is there any relationship between an exciton fusion kinetics model and the KWW function? We investigate these problems by monitoring the triplet kinetics in films of P1VN/PMMA blends as a function of concentration at 77 K.

In this study, the phosphorescence and delayed fluorescence decays are utilized to derive an effective spectral dimension,[16,20] based on a heterofusion kinetics analysis, thereby revealing the effective dimensionality of the triplet transport. We also compare, for dilute blends, the heterogeneity exponents obtained from the modified KWW fit with those from the heterofusion kinetics fit. Intramolecular and intermolecular singlet (and triplet) excimer emission are also studied. An energy funnel distribution may enhance effective triplet trapping, leading to heterofusion based pseudounary kinetics.

Section II of this paper describes the relation of experimental observables and theory. Section III provides the details of our experimental techniques. In section IV, we fit the decays of phosphorescence and delayed fluorescence with a triplet heterofusion model as well as a modified KWW model, yielding the heterogeneity exponents. Section V relates the dynamical topology of the triplet excitation transport to the structural morphology of the blends. Section VI summarizes our conclusions.

II. Relation of Experimental Observables and Theory

The typical reaction of interest is the elementary bimolecular reaction

$$A + A \rightarrow \text{products} \tag{1}$$

and the rate of reaction can be expressed as

$$-d[A]/dt = k[A]^2 \tag{2}$$

where [A] is the reactant concentration, and the rate constant, k, is independent of both concentration and time. The stochastic approach of Smoluchowski[26] and others[27] derives a time-independent rate constant k for long times ($t \rightarrow \infty$), which is proportional to the microscopic diffusion constant D:

$$k \sim D \text{ as } t \rightarrow \infty \tag{3}$$

This approach is based on the assumption that the mean square displacement is linear in time and on having a three-dimensional homogeneous system. However, for low dimensional heterogeneous systems, the self-stirred or diffusion-limited reactions have been shown by simulations[28] to have a rate "constant" that decreases monotonically in time

$$k = k(t) \sim dS/dt \tag{4}$$

where dS/dt is the effective space explored by a random walker in unit time (or the efficiency of the walker).[29]

Specifically, the net exploration space $S(t)$ (or the mean number of distinct sites visited) is a time-dependent microscopic quantity

$$S(t) \sim t^{d_s/2} \qquad d_s < 2 \tag{5}$$

where d_s is the spectral dimension,[30] which for fractal objects is a second dimension in addition to the fractal dimension.[31] The quantity d_s may also be envisaged as an effective dynamic dimension explored by random walkers (here triplet excitons). It may also represent a crossover from one to three dimensions.[20] Substituting eq 5 in (4), the rate constant becomes

$$k(t) \sim (d_s/2)t^{(d_s/2-1)} \sim t^{-h} \qquad 0 \le h \le 1 \tag{6}$$

where

$$h = 1 - d_s/2 \qquad d_s < 2 \tag{7a}$$

while

$$h = 0 \qquad d_s > 2 \tag{7b}$$

Here h can be considered as a heterogeneity exponent, characterizing the transport topologies in a disordered medium. Equation 7b is only valid for a three-dimensional Euclidean homogeneous system. For the borderline case of $d_s = 2$, $h \simeq 0$. When $h > 0$, we call it a fractal-like transport.[20c] This does not necessarily mean that the sample is really a fractal. It could also describe a crossover regime from low to high effective dimensionality.

In practice, delayed fluorescence is generated via the annihilation of two triplet excitons. The rate of triplet depletion, R, is dominated by two decay processes

$$R = R_a + R_n \tag{8}$$

where R_a and R_n are the rate of triplet–triplet annihilation and triplet natural decay, respectively. Combining eq 2, 6, and 8, the rate of triplet depletion can be expressed as

$$-d\rho/dt = k_a t^{-h}\rho^2 + k_n\rho \qquad 0 \le h \le 1 \tag{9}$$

where k_a and k_n are respectively the annihilation rate coefficient and the triplet natural decay rate constant and ρ is the concentration of triplet excitons. In classical three-dimensional homogeneous systems, the rate constant is time-independent and $h = 0$. In the presence of trapped triplets with constant concentration (ρ'), the rate of triplet depletion becomes pseudounary (based on heterofusion)[32] in analogy to electron-hole recombination[33]

$$-d\rho/dt = [k_a' t^{-h} + k_n]\rho \qquad 0 \le h \le 1 \qquad k_a' = k_a\rho' \tag{10}$$

Separating variables and integrating eq 10

$$\rho \sim \exp\{-[(t/\tau_a)^\beta + t/\tau_n]\} \qquad 0 \le \beta \le 1 \tag{11}$$

where

$$\beta = 1 - h \tag{12}$$

where τ_n is the triplet natural lifetime and τ_a can be envis-

$$1/\tau_a = (k_a'/\beta)^{1/\beta} \tag{13}$$

$$1/\tau_n = k_n \tag{14}$$

aged as a characteristic lifetime, which is inversely related to the annihilation rate constant as shown in eq 13.

Equation 11 shows that the concentration of triplet excitons can be indeed expressed as a modified stretched exponential function. For long natural lifetimes ($k_n \rightarrow 0$), it becomes a simple stretched exponential function. The triplet concentration can also be monitored experimentally via phosphorescence decay (I_p), so eq 11 can be rewritten as

$$I_p \sim \exp\{-[(t/\tau_a)^\beta + (t/\tau_n)]\} \tag{15}$$

In the case of heterofusion, if we consider the triplet–triplet annihilation channel only, then eq 10 gives

$$R_a = k_a' t^{-h}\rho \tag{16}$$

where R_a is the annihilation rate that can be monitored

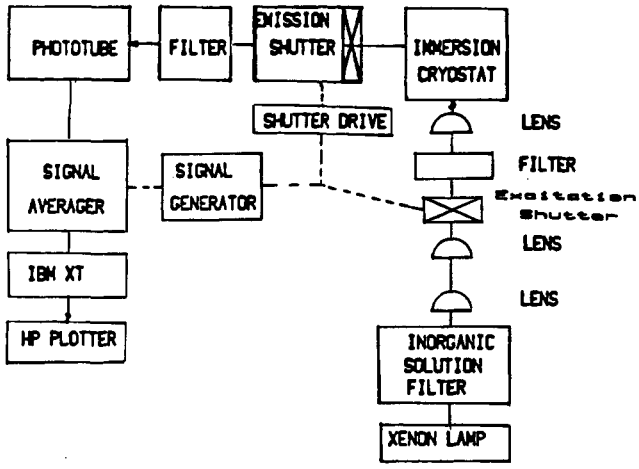

Figure 1. Schematics of apparatus for kinetic measurements.

via delayed fluorescence decay (I_{df}); thus eq 16 can be expressed as

$$I_{df} \sim t^{-h} I_p = t^{(\beta-1)} I_p \tag{17}$$

Substituting eq 15 into 17

$$I_{df} \sim t^{(\beta-1)} \exp\{-[(t/\tau_a)^\beta + (t/\tau_n)]\} \tag{18}$$

Thus, the delayed fluorescence decay can be expressed in terms of a product of an algebraic and a modified stretched exponential function, provided that the triplet–triplet annihilation follows a pseudounary model.

III. Experimental Section

Linear P1VN (MW ≃ 100 000) and PMMA (MW ≃ 154 000) obtained from Polyscience was further purified by multiple reprecipitation with spectral graded dichloromethane and methanol as a solvent and non-solvent pair. Films of P1VN and PMMA blends are prepared by the solvent casting technique except for the 100% P1VN powder sample. Polymers are first weighed and dissolved in dichloromethane, then vigorously stirred for several hours in a dry nitrogen glove box. The films (thickness in the range of 35–45 μm) are cast by using the doctor blade technique.[34] The most dilute film (0.8%) looks the most transparent. Going to 2% the scattering definitely increases, but the film still appears transparent to the eye. At 5% the film looks translucent and the degree of opaqueness increases monotonically, reaching total opaqueness at about 16%. The 100% P1VN is in white powder form. Fresh samples subject to no previous irradiation were used for this study. The samples are mounted on a sample holder and transferred to an immersion cryostat filled with liquid nitrogen.

Steady-state emission is measured with the sample oriented 45° to the incident excitation and with detection at the back face. No differences in the emission spectra is observed upon detection at the front face. A 1600-W Hanovia xenon arc lamp with water-cooled inorganic solution filter and appropriate bandpass filters was used as a 290 ± 10 nm excitation light source. The emission is collected with a six-element compound (relay) lens specially manufactured by Karl Lambrecht Corp. and is focused on the slits of a Model 25-100 Jarrell-Ash spectrometer of 1.0-m focal length. Its gratings have 1180 grooves/mm, with an overall resolution of 8 Å/mm slit width in first order. The emissions are detected with an ITT F-4013 photomultiplier tube (cooled to −25 °C), using a Princeton Applied Research (PAR) Model 1120 discriminator and a Model 1110 photon counter. Spectra are recorded with an IBM XT microcomputer, which is interfaced with the photon counter and spectrometer. All emission spectra shown in this study are not corrected for phototube response. Both data acquisition and analysis are driven with ASYST manufactured by Macmillan Software Co.

For kinetic measurements under steady-state excitation, Figure 1 shows the schematic diagram of detecting slow delayed fluorescence and phosphorescence decays. The excitation shutter (Uniblitz) controlling the duration of incident excitation is triggered to close, while the emission shutter (in front of phototube) is triggered to open and the signal averager (PAR 4202H) starts sampling. A delay of ~10 ms between the two shutters is generated to cutoff all prompt fluorescence. The data is then transferred and stored in the IBM XT. Delayed fluorescence and phosphorescence decays are isolated respectively by placing Hoya-U330 and Corning-369 filters in front of the phototube.

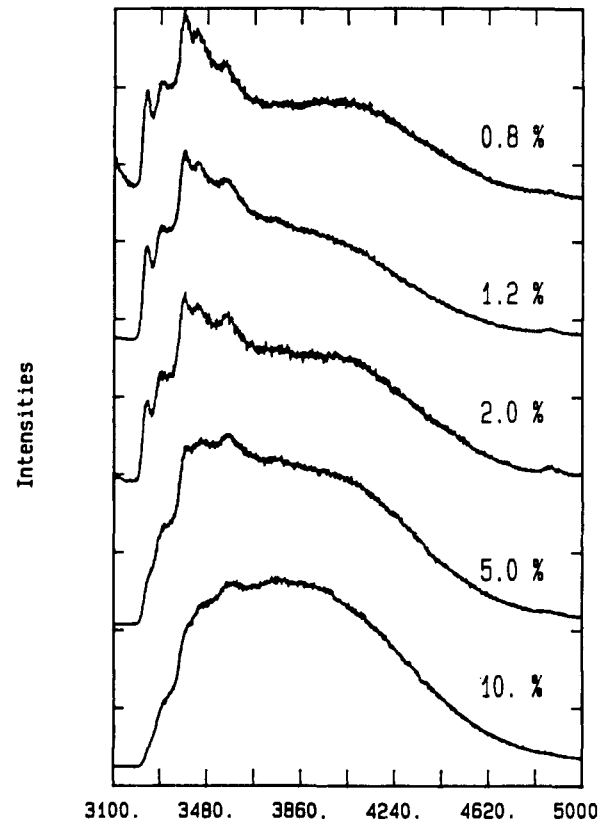

Figure 2. Normalized steady-state emission spectra of P1VN/PMMA at 77 K (spectra are offset successively).

A Perkin-Elmer differential scanning calorimeter, Model DSC 7, was used in conjunction with a Perkin-Elmer 7700 data station and a TAC 7/7 controller to study the glass transition of the blends. The heating and quenching rate are respectively 10 and 200 °C/min. The range of temperature scanned is 50–180 °C.

IV. Results and Discussion of Excitation Fusion Kinetics

Figures 2 and 3 show the fluorescence spectra from 0.8 to 100 wt % of P1VN/PMMA blends under steady-state excitation of 290 ± 10 nm at 77 K. The emissions in the range of 320–480 nm are composed of both prompt and delayed fluorescence. As the concentration of P1VN increases, the singlet excimer emission (with peak maximum at ~400 nm) increases at the expense of monomer fluorescence (with peak maximum at ~333 nm). The samples are thin enough (~40 μm) to minimize reabsorption in the monomer spectral region.

In dilute samples, below 16%, the singlet excimer tails are overlapped with monomer phosphorescence between 480 and 500 nm, which is shown better in Figure 4. The peak maximum at 488 nm is monomer phosphorescence, which is not observed above 10%. Peaks at 530 and 570 nm may be, respectively, attributed to the shallow and

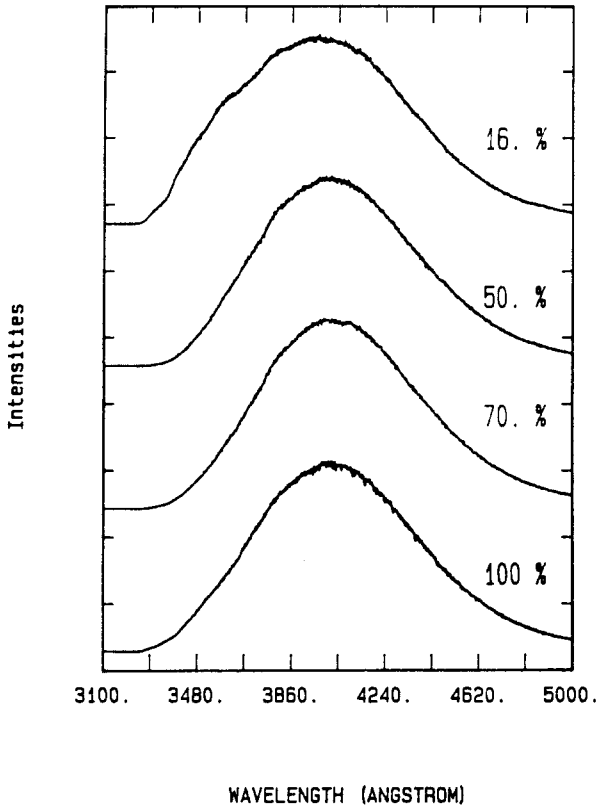

Figure 3. Normalized steady-state emission spectra of P1VN/PMMA at 77 K (spectra are offset successively).

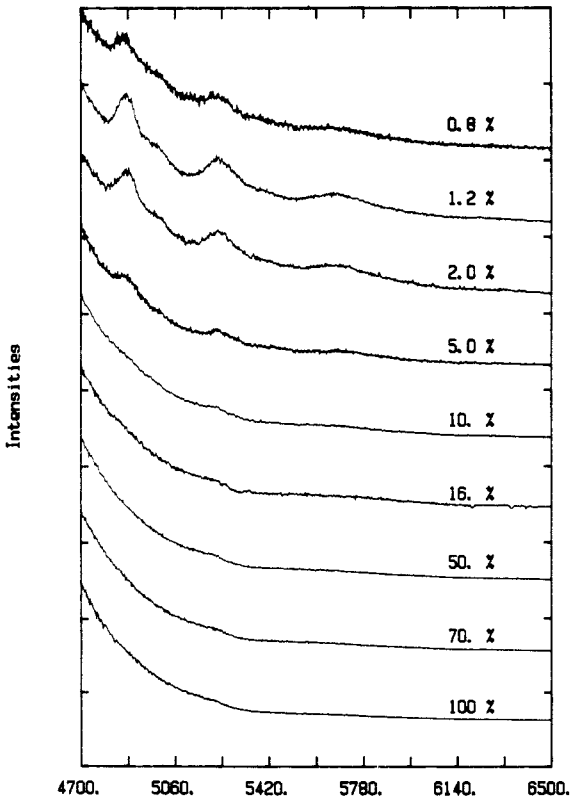

Figure 4. Normalized steady-state emission spectra of P1VN/PMMA at 77 K at longer wavelengths (spectra are offset successively).

deep triplet excimer traps.[35] The energy of the P1VN triplet excimer (18 870 and 17 540 cm^{-1}) also agrees with the naphthalene triplet excimer energy reported earlier.[36] The excimer peaks are overlapped with monomer

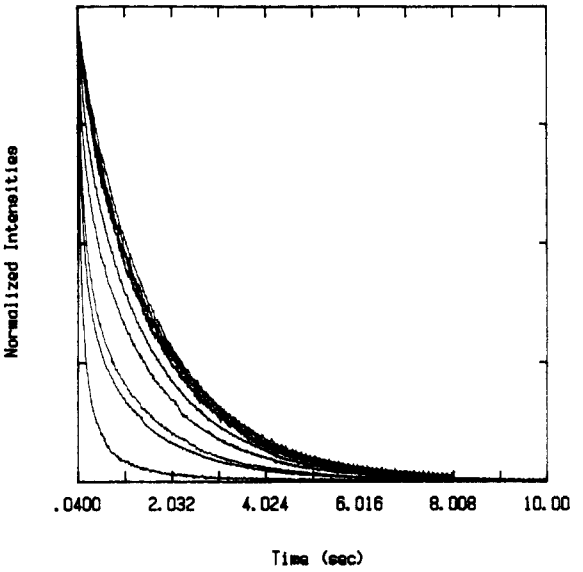

Figure 5. Normalized phosphorescence decays of P1VN/PMMA at 77 K (top to bottom: 0.8, 1.2, 2.0, 5.0, 10, 16, 50, 70, and 100%).

phosphorescence vibronic peaks in dilute samples below 10%. However, in concentrated samples, the triplet excimer peaks are obscured by the overlapping with strong singlet excimer tail.

Excimer formation P1VN was reported[1] to be largely intramolecular and probably results from interaction between adjacent chromophores on the polymer chain, while interchain excimers are also formed in concentrated samples. This supports the suggested excimer formation mechanism[37] that excitation energy migrates through the chromophores of a polymer chain until a site favorable to excimer formation is encountered.

Intramolecular excimer formation in linear aryl vinyl polymers is highly favorable, since their adjacent chromophores have separations on the order of 3–4 Å and a long sequence of closely spaced pendent groups can reorient to form excimer sites. Thus, even at a concentration as low as 0.8%, excimer emissions are still observed, originating from intrachain stackings. Obviously, in concentrated blends, both intrachain and interchain stackings are possible as implied in the increase in excimer to monomer intensity ratio.

Figures 5 and 6 show respectively the normalized phosphorescence and delayed fluorescence decays at 77 K for various weight percents of P1VN. As the P1VN concentration increases, higher connectivity can be achieved, leading to faster decays and transport. Figure 6 shows the delayed fluorescence decay curves only up to 16%. As the concentration increases above 16%, the decays at early times (<1 s) are relatively unchanged but appear to have a slowly decaying component at longer times.

Figure 7 shows the linear slope of $-h$ obtained by plotting ln $[I_{DF}/I_p]$ versus ln [time] for 2, 10, and 50% samples. In contrast, a clearly nonlinear behavior is found on replacing I_p with I_p^2 in the fittings, suggesting that the triplet–triplet annihilation kinetics follows pseudounary fusion (heterofusion) kinetics as given in eq 16 and 17, at least within the first approximation. In addition, all samples under investigation have been shown to follow such pseudounary heterofusion kinetics. The uncertainty with respect to the slope is about 20–30%. The most obvious characterization of the differences among the samples is in terms of the slope "$-h$", i.e., the heterogeneity exponent, h. Figure 8 shows the concentration

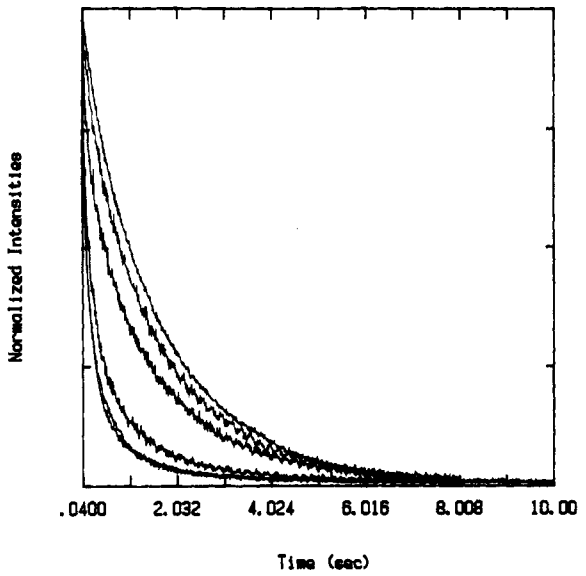

Figure 6. Normalized delayed fluorescence decays of P1VN/PMMA at 77 K (top to bottom: 0.8, 1.2, 2.0, 5.0, 10, and 16%).

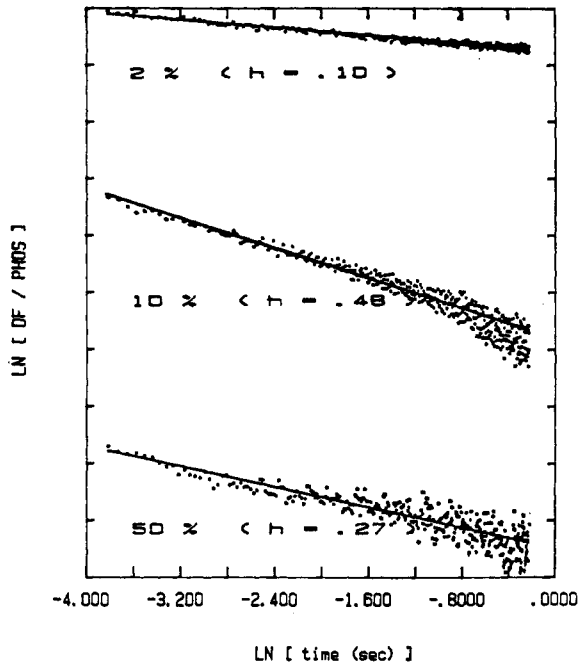

Figure 7. Determination of heterogeneity exponents of P1VN/PMMA from linear least-squares fit. Note that each division of the vertical axis is 0.59 unit and that each curve is offset vertically for purpose of clarity.

dependence of the heterogeneity exponent, which is also given in Table I.

In spite of chain isolation in dilute films, excimers still exist. This has been studied in detail in similar systems and attributed to the formation of intramolecular excimers (mostly among adjacent chromophores).[12-14] The heterofusion model obviously suggests a fairly effective trapping mechanism for the triplet excitons. Temperature dependence studies of delayed emission of P1VN solid films[35] reveal that the triplet excimers responsible for the 530 and 580 nm emission are shallow and deep traps, respectively. The triplet excitons are trapped only momentarily in the shallow traps. The deep traps, however, may be envisaged as an energy funnel with a large cross section, effectively sucking in all nearby triplets. Thus, the deep traps are always populated with a constant concentration, leading to the pseudounary fusion kinetics (eq 16). We note that the total triplet exciton

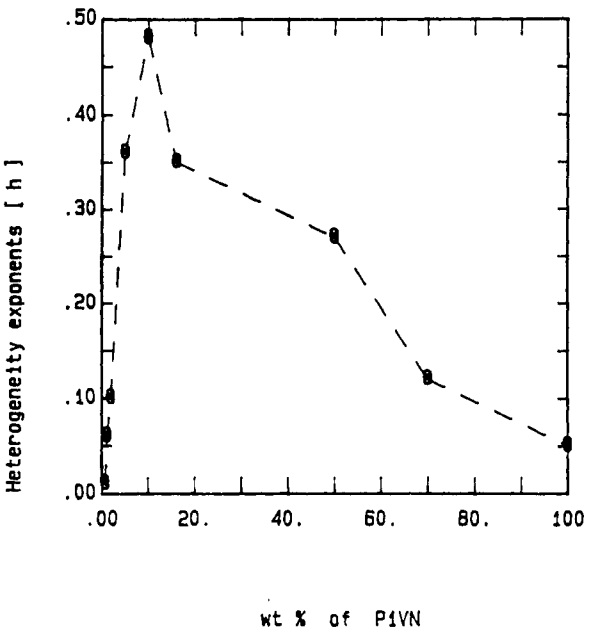

Figure 8. Weight percent dependence of heterogeneity exponents in P1VN/PMMA at 77 K.

Table I
Heterogeneity Exponents (h) of P1VN/PMMA

wt %	[h]	wt %	[h]
0.8	0.01	16	0.35
1.2	0.06	50	0.27
2.0	0.10	70	0.13
5.0	0.36	100	0.05
10.0	0.48		

population is less than 10^{-4} excitons per chromophore.[38] On the basis of the 10% fluorescence spectrum, the fraction of singlet excimer forming sites is of the same order of magnitude as that estimated by Frank and Harrah for 0.2% P2VN in PS,[39] i.e., 10^{-2} excimer forming sites per chromophore. With the assumption of a similar fraction for triplet excimer forming sites, then within the time scale of 1 ms to 1 s, the great majority of triplet excitons is trapped excitons, e.g., excimers. These rough estimates of exciton and excimer forming site populations are thus consistent with heterofusion dominating over homofusion. This predominance in the triplet state of trapped excitons over mobile excitons is also consistent with the observed triplet spectra. We note that such a fraction of excimer forming sites (10^{-2}) combined with the triplet excimer to monomer intensity ratio ($10-10^2$) gives an estimated exploration range of about 10^3 Å.

As the P1VN concentration decreases below 2%, h approaches zero, indicating that k is time-independent. The long and comparable lifetimes of the delayed fluorescence and phosphorescence for the 0.8% sample suggest that the depletion of the isolated excitons is either by phosphorescence or by tunnelling among traps, resulting in annihilation. In the presence of deep traps, intrachain and interchain exciton tunnelling among energy funnels is still possible, apparently leading to reaction-limited rather than diffusion-limited transport. We also note that between 2% and 5%, we find a crossover to a diffusion-limited regime (see below).

From 5 to 50%, a strong time dependence of the rate constant is reflected in the nonzero h values, showing that the triplet transport is definitely diffusion-limited. At ~10%, h = 0.48 and d_s = 1.04, suggesting that the tenuous connectivity among P1VN chains leads to ramified, quasi-one-dimensional networks.[16] In other words,

the chains are effectively longer in comparison with those in dilute blends. As intermolecular contact occurs, the dimensionality of energy migration increases from one-dimensional to three-dimensional with a consequent increase in efficiency of excimer sampling.[3a] Above 50%, interchain connectivity is high enough for enhanced homogeneous (isotropic) exciton diffusion and thus approximately gives a classical time-independent k with h close to zero. In principle, the triplet transport can now be reaction-limited and/or diffusion-limited, since both quantum tunnelling and random walking of triplet excitons in such high dimensional media will give the classical kinetics result.

In classical three-dimensional homogeneous systems, excited chromophores are created at random, and the exciton diffusion is sufficient to well stir them and give a random distribution. Thus, no time dependence in the rate constant is ever observed. In other words, the extent of the population randomness is invariant in time, although the size of the triplet population decreases in time.[38]

However, in disordered heterogeneous systems, the initial exciton distribution created (immediately after the long-time incident excitation is shut) is not uniformly random, since excitons in close proximity annihilate almost instantly. Only those that are further apart from each other as well as in "hidden" areas can survive. Thus, the topological disorder in the heterogeneous systems can be reflected by a nonrandom time-dependent exciton distribution.[20c] At long times, the excitons become even more isolated rather than having a uniformly random distribution. The heterogeneity exponent, h, can then be used to characterize the deviation from randomness of the triplet exciton distribution.

In Table I, the highest h value (0.48) of the 10% sample suggests the largest deviation from randomness of the exciton distribution among all the samples. However, for concentrated samples (>70%), the higher connectivity and the shorter relative distances among the chromophores greatly enhance the exciton diffusion, resulting in an effectively random exciton distribution. Similarly, for dilute blends, since the guest P1VN chains are mostly isolated and transport is largely intramolecular,[1] the exciton distribution among chains is determined by the random absorption of light quanta and thus, for different reasons, is expected to be close to uniformly random, i.e., a statistical distribution (provided that we consider only those regions which the triplet excitons are able to visit).

Furthermore, the application of a weighted sum of two exponentials to the decays of delayed fluorescence and phosphorescence, with *three* fitting parameters *for each*, fails to give a reasonable fit.[38] The modified stretched exponential function is also applied to fit the nonexponential delayed fluorescence and phosphorescence at 10% P1VN as shown in Figure 9. Equation 11 is used to fit the phosphorescence decays from 0.8 to 10%, where τ_a and β are the *two fitting parameters* and τ_n is the natural lifetime of naphthalene (2.2 s)[19c] as given in Table II. For concentrations higher than 10%, the modified stretched exponential model fails to give a reasonable fit. Below 10%, τ_a and β increase as the concentration decreases (except β_p for 0.8%). At 0.8%, $\tau_a \sim 8$ s, $\beta \sim 1$, and $k_a' \simeq 0.125\ s^{-1}$. It is obvious that as β approaches 1, the relaxation distribution tends to be a single exponential. We note that the phosphorescence may also represent, in part, regions with no exciton mobility, i.e., trapped excitons. The delayed fluorescence (see below) may thus be a more refined kinetic tool.

Equation 18 is used to fit the delayed fluorescence decays

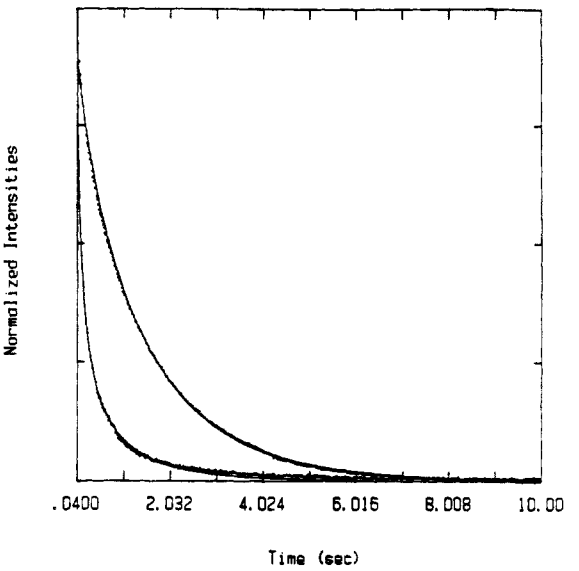

Figure 9. Modified stretched exponential fit of 10% P1VN/PMMA at 77 K. The top curve is the phosphorescence (dotted line) fitted to eq 11, with β_p and τ_a as free parameters (solid line). The bottom curve is the delayed fluorescence (dotted line) fitted to eq 18, with a single parameter, β_{df} (solid line). See text.

Table II
Stretch-Exponential Fit of P1VN/PMMA[a]

wt % of P1VN	τ_a	β_p	β_{df}	$[h]^a$	$[h]_t$
0.8	8.46	0.89	0.98	0.02	0.01
1.2	8.01	0.94	0.96	0.04	0.06
2.0	7.26	0.91	0.88	0.12	0.10
5.0	5.96	0.89	0.63	0.37	0.36
10.0	4.46	0.79	0.51	0.49	0.48

[a] $[h]$ obtained from $(1 - \beta_{df})$. [b] $[h]_t$ obtained from Table I.

from 0.8 to 10%, where β is the *only fitting parameter*, as the τ_a values are obtained from the phosphorescence fits. At 10% concentration, there is a slight deviation at long times, but the fit at early times is reasonably good as shown in Figure 9. Again below 10%, β increases as concentration decreases. β is related to h as given in eq 12, and agrees very well with the h value obtained from the ln–ln plots as shown in Table II. The linear relationship between h and β for dilute samples can also be seen in Figure 10. We note that the line is the theoretical expectation ($\beta = 1 - h$). Above 10%, the modified stretched exponential function no longer fits the decays, probably due to the complicated kinetics resulting from intermolecular transport.

While the heterogeneity exponent $[h]$ may serve to characterize the dimensionality of the exciton transport as well as the topological disorder, these $[h]$ values also depict a clear excitation intensity dependence as shown in Figure 11. Neutral density filters are added to attenuate the incident excitation intensity for the 10% sample. The $[h]$ values in general vary linearly or monotonically with the excitation intensity.

The highest experimentally accessible excitation intensity ($\sim$1.0 arbitrary unit) shows $h = 0.48$ and $d_s = 1.04$; indicating that the transport is quasi-one-dimensional. Extrapolating to zero excitation intensity, $h \simeq 0.24$ and $d_s \simeq 1.52$, suggesting a fractal-like transport. Higher excitation intensity can generate more excitons (in a single chain) with a relatively shorter average distance between them. This leads to faster decays and more efficient intramolecular annihilation. It emphasizes the one-dimensional transport topology. In contrast, lower excitation intensity can dramatically decrease the number

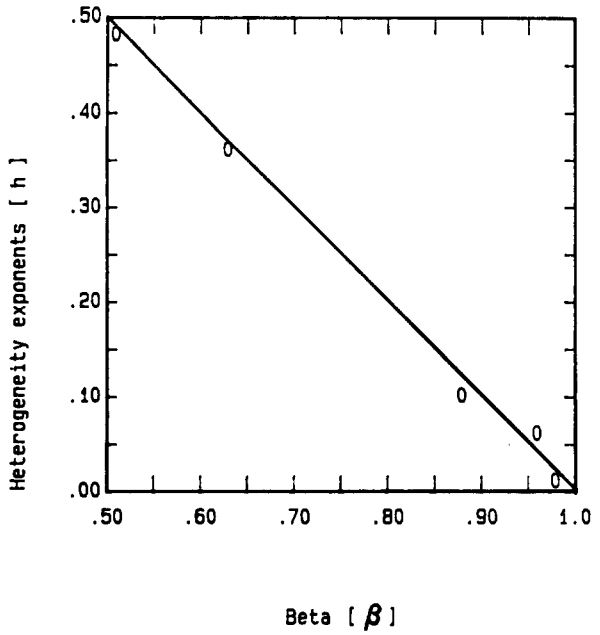

Figure 10. Relationship between heterogeneity exponents [h] and critical exponent [β] of P1VN/PMMA at 77 K. The line is from theory (eq 12).

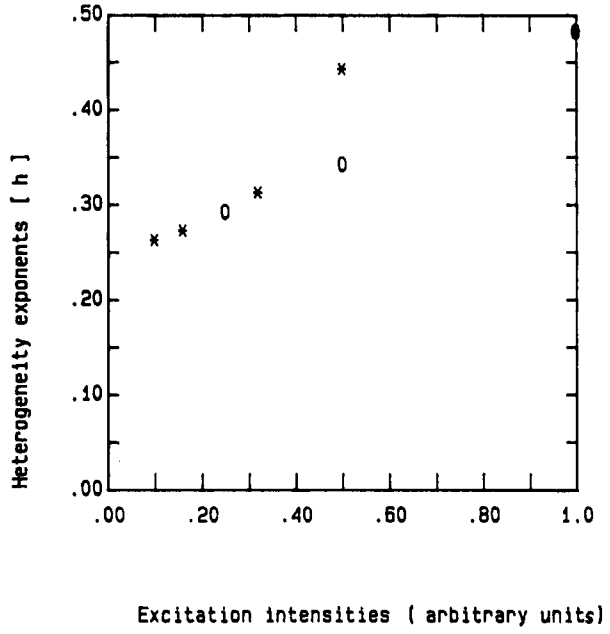

Figure 11. Excitation intensity dependence of heterogeneity exponents of 10% P1VN/PMMA at 77 K (asterisks and squares represent the h values obtained from two separate regions of the sample).

of separated excitons (per chain), so that excitons may need to hop among the tenuously connected chains in order for annihilation to take place. Indeed, decreasing the excitation intensity could have similar effects on transport as the lowering of concentration of chromophores. Similar effects are also observed in excitation duration studies.[38,40,41]

Temperature studies, from 77 K up to ~150 K, show no significant changes in the heterogeneity exponent, h (but do show a weakening in luminescence intensity—for details see ref 38). We thus attribute the kinetic fractal-like effects predominantly to geometrical (morphological) constraints rather than to energetic disorder.[18-25]

At much higher temperatures (325–450 K), DSC measurements of all the fresh films show some anomalous endothermic peaks on the *first* scan, probably indicating a distribution of nonequilibrium states. When the films are fast quenched from a temperature above the glass transition temperatures (T_g) of the pure components (i.e., 450 K), a single T_g appears consistently for all dilute films (<16%) on the *second* scan. However, a very weak shoulder shows up in the glass transition for the 50% and 70% blends, suggesting partial miscibility rather than total segregation.

Spectroscopic studies of the fast-quenched blends were also performed.[38] Qualitatively, there are changes in the emission spectra, decay times, and heterogeneity exponents. For the concentrated blends of 50% or higher, because of their short decay times, no complete analysis of h is possible with the current instrumentation. However, at dilute concentrations, one observes a consistent reduction in h for all the fast-quenched samples, but still showing the same pattern of concentration dependency as before (i.e., increasing monotonically from 1% to 10% and then decreasing again). The local heterogeneity of the sample is thus decreased. Concomitantly, higher ratios of singlet excimer to singlet monomer intensity in the fluorescence spectra are also observed and are consistent with faster singlet diffusion in the fast-quenched samples, again resulting from more homogeneous samples. In addition, the faster decays observed in the fast-quenched samples also suggest faster triplet–triplet annihilation, as a consequence of faster triplet diffusion, thus providing a third indication that the samples become locally homogeneous after thermal treatment. The exciton transport studies are consistent with the qualitative expectations from the thermal treatment (see section V). A quantitative analysis will be reported on separately.

V. Excitation Transport Topology and Structural Morphology

Our delayed fluorescence results are not inconsistent with the prompt fluorescence results.[1-5] The latter relate to singlet energy transport, while the former relate to triplet energy transport. The singlet excitation transfer occurs via transition-dipole–transition-dipole interactions (as well as higher multipoles) operating over a range of 20–100 Å, while the triplet transfer involves exchange interactions operating over 5–20 Å.[42] The former interactions thus have a much longer range than the latter. Singlet excitation transfer can therefore be utilized to find the radius of gyration of the polymer.[5] On the other hand, triplet transfer (single jump) is limited to very short distances (except for infrequent tunnelling). It can thus proceed only along the chain, between adjacent chromophores, except for real "short circuits".[3a] A "short-circuit" is considered to be a situation where nonadjacent chromophores get as near to each other as adjacent chromophores. We note, however, that the long triplet lifetime allows for a large number of jumps. Triplet exciton transfer is therefore more closely related to the direct chemical connectivity (primary and tertiary) of the polymers, while singlet transfer is a measure of the medium-range topology. Ideally, studies of triplet and singlet excitation transfer should be employed in complementary fashion, but we do not expect to have a one-to-one correspondence in their transfer rates and transfer topology. We also note that the triplet studies significantly extend the range of blend composition that can be studied by excitation transport. While the fluorescence spectra are practically unchanged from 16% to 100% P1VN, the triplet exciton kinetics continue to be informative throughout the entire composition range.

The exciton transport behavior, as expressed by h or β, shows a *continuous and reproducible dependence on*

concentration (see Figure 8). The same is true for the spectra (Figures 2–4). For the pure P1VN phase in the blends, we expect to have $h = 0$ and no monomeric features in the emission spectrum. There is, therefore, *no evidence for a sudden total segregation of P1VN and PMMA*. Moreover, the h values of the blends cannot be explained in terms of a superposition of the dilute and concentrated phases (both having $h = 0$), as is evident for the 10% blend ($h = 0.5$). Rather, the morphology of each blend composition is clearly reflected by the triplet excitation transport topology. The dilute blends appear to consist partially of quasi-isolated chains with a quasi-one-dimensional chromophore morphology (on a monomer length scale); i.e., there is no compact aggregation or compact globule formation of P1VN chains. Specifically, the triplet exciton transport topology is indeed consistent with isolated random coils but neither with isolated compact guest coils nor with guest–guest interpenetrating random coils, which would lead to zero h values and to strictly excimeric spectra. The chains of the dilute polymer are thus more ramified than compact.[16] They do interpenetrate with host chains but are mostly isolated from each other. While the information on the higher concentration range (16–100%) does not provide a complete topological picture, it does provide specific constraints. For instance, it is *inconsistent with sudden or complete phase segregation.*

For the more dilute blends (0.8–2%) we have stated in section IV that the kinetics is reaction-limited rather than diffusion-limited. Reaction-limited kinetics is always classical, i.e., $h = 0$, for all dimensionalities. Thus, we cannot draw any conclusions regarding transport topology from the exciton fusion kinetics of these samples. However, the monomer–excimer ratios are consistent with the existence of some isolated, or partially isolated P1VN chains. Indeed recent pulsed laser studies[43] show h increasing to 0.5 for diffusion-limited kinetics at concentrations below 0.05%.

We digress to discuss two idealized models. (1) The first is a thermodynamically totally miscible blend of two glassy polymers that would have a nearly random distribution of polymer chains (not to be confused with exciton distribution). Such a blend would be optically clear and globally (macroscopically) homogeneous; however, locally (microscopically) it would be heterogeneous. (2) On the other hand, a totally immiscible blend would appear to be optically nontransparent and macroscopically heterogeneous. However, this blend would have a locally segregated morphology, having microscopically homogeneous regions of either one or the other pure components. Hence, it is important not to confuse local with global homogeneity (or heterogeneity).

Our heterogeneity exponent, h, monitors the *local geometric disorder*, while other methods such as DSC and optical clarity only refer to the global property. The DSC results suggest partial miscibility in the fast-quenched 50% and 70% P1VN/PMMA. As stated above, the thermal treatment of the fresh films reduces h and increases the excimer to monomer fluorescence ratio. Both these facts do suggest an increase in local homogeneity due to thermal treatment. This may be due to thermally induced phase segregation (which is consistent with the DSC results on the fast-quenched samples).

VI. Summary and Conclusions

The triplet–triplet annihilation of P1VN/PMMA blends at 77 K is found to follow pseudounary (heterofusion) kinetics, in which deep excimer traps have a constant population and shallow excimer traps are considered to be capable of trapping mobile triplets only momentarily. Although the heterogeneity exponent h increases somewhat with the excitation intensity, it clearly shows a strong and consistent dependence on the concentration of the chromophores. Whether it really indicates a fractal topology or just a crossover from one-dimensional to classical behavior remains to be established. However, when h is in the vicinity of 0.5, rather than zero, this points strongly toward quasi-one-dimensional guest (P1VN) networks. From this one may argue further about the morphology of the polymer blend in the given film sample.

Unlike classical kinetics in homogeneous media, fractal-like kinetics in heterogeneous media allows us to easily distinguish between reaction-limited and diffusion-limited reactions via the time dependence of the rate constant. At concentrations below 2%, the rate constant is time-independent and we suggest that the triplet transport is reaction-limited and probably involves intrachain and/or interchain quantum mechanical tunnelling. As the concentration increases above 2%, both quantum tunnelling and random walking processes are competing with each other, giving rise to an increasing time dependence of the rate coefficient. The crossover to quasi-one-dimensional, diffusion-limited transport happens to be at about 10% weight, implying that P1VN chains are tenuously connected and that intermolecular transport becomes more favorable, compared to the more dilute samples (however, transport is still predominantly intrachain). Above 10%, relatively high connectivity is achieved, and the transport is no longer dominated by intramolecular transfer but significantly influenced by intermolecular transfer. The increased isotropic nature of the transfer reduces the time dependence of the rate coefficient. Above 70%, again no time dependence is observed in the rate constant, and the triplet annihilation could be a classical diffusion-limited reaction or, alternatively, a reaction-limited reaction.

Only for 0.01% and lower concentration samples do the P1VN chains form a truly one-dimensional environment, i.e., isolated chains.[43] At higher concentrations (about 1%) there is some aggregation followed by segregation. However, at still higher concentrations, the segregation domains (of P1VN) may be surrounded by a "fuzz" (a region where P1VN chains stick out of their domains, as if the compact P1VN regions grow P1VN "hair" that protrudes around them). Such defective domain boundaries have been observed before for vapor-deposited naphthalene films.[44]

The modified stretched exponential formalism of phosphorescence and delayed fluorescence decays serves as an excellent probe for the heterogeneity of disordered media. It also is an excellent criterion for distinguishing between diffusion-limited and reaction-limited kinetics in heterogeneous media. Furthermore, triplet exciton migration is a very sensitive tool, elucidating the finest, short-range details of the polymer blend morphology. The chromophore excitation topology follows closely the isolated chain morphology for the dilute P1VN blends. It seems thus to *exclude compact globule formation and a tight aggregation of P1VN chains.* Furthermore, in contrast to singlet excimer studies, the triplet kinetics also provide information on the medium and high concentration blends. Thus, for our nonequilibrium cast films, for which the DSC procedures are destructive and the optical clarity tests are not very conclusive, the combined triplet and singlet exciton kinetics approach appears to provide some significant morphological information.

Note Added in Proof. Further studies using laser excitation (Z.-Y. Shi and R. Kopelman) confirm and extend most of the results of this paper. The only difference is for the 0.8% and 1.2% samples, where $h > 0$. However, the decrease of h from 10% to 2% is confirmed and appears to be a highly interesting topological effect.

Acknowledgment. This work was supported by the National Science Foundation under Grant No. DMR-8801120.

References and Notes

(1) Fox, R. B.; Price, T. R.; Cozzens, R. F.; McDonald, J. R. *J. Chem. Phys.* **1972**, *57*, 534.
(2) (a) Gelles, R.; Frank, C. W. *Macromolecules* **1982**, *15*, 1486. (b) Gelles, R.; Frank, C. W. *Macromolecules* **1983**, *16*, 1448. (c) Frank, C. W.; Gelles, R. In *Photophysical and Photochemical Tools in Polymer Science*; Winnik, M. A., Ed.; D. Reidel: Boston, 1986; NATO ASI Series, Vol. C182, p 561.
(3) (a) Frank, C. W.; Gashgari, M. A. *Ann. N.Y. Acad. Sci.* **1981**, *366*, 387. (b) Frank, C. W.; Gashgari, M. A.; Semerak, S. N. In *Photophysical and Photochemical Tools in Polymer Science*; Winnik, M. A., Ed.; D. Reidel: Boston, 1986; NATO ASI Series, Vol. C182, p 523.
(4) Morawetz, H. *Ann. N.Y. Acad. Sci.* **1981**, *366*, 404; *Science* (Washington, DC) **1988**, *240*, 172.
(5) (a) Fayer, M. D. *J. Lumin.* **1984**, *31*, 525 and references therein. (b) Peterson, K. A.; Fayer, M. D. *J. Chem. Phys.* **1986**, *85*, 4702. (c) Peterson, K. A.; Zimmt, M. B.; Linse, S.; Dominque, R. P.; Fayer, M. D. *Macromolecules* **1987**, *20*, 168.
(6) Kim, N.; Webber, S. E. *Macromolecules* **1980**, *13*, 1233.
(7) (a) Pasch, N. F.; Webber, S. E. *Chem. Phys.* **1976**, *16*, 361. (b) Klopffer, W.; Fischer, D.; Naundorf, G. *Macromolecules* **1977**, *10*, 450.
(8) Holden, D. A.; Ren, X. X.; Guillet, J. E. *Macromolecules* **1984**, *17*, 1500.
(9) Ghiggino, K. P.; Roberts, A. J.; Phillips, D. *Adv. Polym. Sci.* **1981**, *40*, 69.
(10) Phillips, D.; Roberts, A. J.; Souta, I. *J. Polym. Sci., Polym. Phys. Ed.* **1982**, *20*, 411.
(11) Phillips, D.; Roberts, A. J.; Soutar, I. *Polymer* **1981**, *22*, 427.
(12) (a) Fitzgibbon, P. D.; Frank, C. W. *Macromolecules* **1982**, *15*, 733. (b) Semerak, S. N.; Frank, C. W. *Can. J. Chem.* **1985**, *63*, 1328.
(13) Gelles, R.; Frank, C. W. *Macromolecules* **1982**, *15*, 741.
(14) Fredrickson, G. H.; Frank, C. W. *Macromolecules* **1983**, *16*, 572.
(15) Kauffmann, H.; Weixelbaumer, W. D.; Buerbaumer, J.; Mollay, B. *J. Chem. Phys.* **1986**, *85*, 3566.
(16) Kopelman, R. *J. Stat. Phys.* **1986**, *42*, 185. Stauffer, D. *Introduction to Percolation Theory*; Taylor and Francis: London, 1985.
(17) (a) Blumen, A.; Klafter, J.; Zumofen, G. In *Optical Spectroscopy of Glasses*; Zschokke, I., Ed.; D. Reidel: Boston, 1986; p 199. (b) Richert, R.; Bassler, H. *J. Chem. Phys.* **1986**, *84*, 3567. (c) Richert, R.; Ries, B.; Bassler, H. *Philos. Mag. B* **1984**, *49*, L25.
(18) (a) Bendler, J. T. *J. Stat. Phys.* **1984**, *36*, 625. (b) Bendler, J. T.; Le Grand, D. G.; Olszewski, W. V. In *Transport & Relaxation in Random Materials*; Klafter, J., Rubin, R. J., Shlesinger, M. F., Eds.; World Scientific: Singapore, 1986; p 240. (c) Di Marzio, E.; Sanchez, I. C. In *Transport & Relaxation in Random Materials*; Klafter, J., Rubin, R. J. Shlesinger, M. F., Eds.; World Scientific: Singapore, 1986; p 253.
(19) (a) Newhouse, E. I.; Kopelman, R. *J. Lumin.* **1984**, *31/32*, 651. (b) Newhouse, E. I.; Kopelman, R. *Chem. Phys. Lett.* **1988**, *143*, 106. (c) Newhouse, E. I. Ph.D. Thesis, The University of Michigan, 1986.
(20) (a) Kopelman, R.; Parus, S.; Prasad, J. *Phys. Rev. Lett.* **1986**, *56*, 1742. (b) Kopelman, R.; Prasad, J. *Phys. Rev. Lett.* **1987**, *59*, 2103. (c) Kopelman, R. *Science (Washington, DC)* **1988**, *241*, 1620.
(21) (a) Klymko, P. W.; Kopelman, R. *J. Phys. Chem.* **1983**, *87*, 4565. (b) Newhouse, J. S.; Kopelman, R. *J. Chem. Phys.* **1986**, *85*, 6804.
(22) Kohlrausch, R. *Pogg. Ann. Phys.* **1854**, *91*, 198.
(23) Williams, G.; Watts, D. C. *Trans. Faraday Soc.* **1971**, *66*, 80.
(24) (a) Moynihan, C. T.; Lesikar, A. V. *Ann. N.Y. Acad. Sci.* **1981**, *371*, 151. (b) Patterson, G. D. *Adv. Polym. Sci.* **1983**, *48*, 127. (c) Ngai, K. L. *Comments Solid State Phys.* **1979**, *9*, 127. (d) Shlesinger, M. F. *J. Chem. Phys.* **1979**, *70*, 4813.
(25) Klafter, J. T.; Shlesinger, M. F. *Proc. Natl. Acad. Sci. U.S.A.* **1986**, *83*, 848.
(26) Smoluchowski, M. V. *Z. Phys. Chem.* **1917**, *92*, 129.
(27) Calef, D. F.; Deutch, J. M. *Annu. Rev. Phys. Chem.* **1983**, *34*, 493.
(28) Argyrakis, P.; Kopelman, R. *J. Phys. Chem.* **1987**, *91*, 2699.
(29) (a) Argyrakis, P.; Kopelman, R. *Chem. Phys. Lett.* **1979**, *61*, 187. (b) De Gennes, P. G. *C.R. Acad. Sci., Ser. A* **1983**, *296*, 881.
(30) Alexander, S.; Orbach, R. J. *J. Phys., Lett.* **1982**, *44*, L13.
(31) Mandelbrot, B. B. *The Fractal Geometry of Nature*; W. H. Freeman: San Francisco, 1983.
(32) (a) Gentry, S. T.; Kopelman, R. *J. Chem. Phys.* **1984**, *81*, 3014, 3022. (b) Prasad, J.; Kopelman, R. *Phys. Rev. Lett.* **1987**, *59*, 2103.
(33) Kittel, C. *Introduction to Solid State Physics*; 3rd ed.; Wiley: New York, 1967, Chapter 17.
(34) Allen, E. O. *Plastics Polymer Science and Technology*; Wiley: New York, 1982; p 600.
(35) Burkhart, R. D.; Aviles, R. G.; Magrini, K. *Macromolecules* **1981**, *14*, 91.
(36) Lim, E. C. *Acc. Chem. Res.* **1987**, *20*, 8.
(37) (a) Vala, M. T.; Haebig, J.; Rice, S. A. *J. Chem. Phys.* **1965**, *43*, 886. (b) Hirayama, F.; Basile, L. J.; Kikuchi, C. *Mol. Cryst.* **1968**, *4*, 83.
(38) Li, C. S. Ph.D. Thesis, The University of Michigan, 1988.
(39) Frank, C. W.; Harrah, L. A. *J. Chem. Phys.* **1974**, *61*, 1526.
(40) Kopelman, R.; Parus, S. J. In *Fractal Aspects of Materials II*; Schaefer, D. W., Laibowitz, R. B., Mandelbrot, B. B., Liu, S. H., Eds.; Mat. Res. Soc.: Boston, 1986; p 50.
(41) Kopelman, R. In *Fractal Aspects of Materials III*; Hurd, A. J., Weitz, D. A., Mandelbrot, B. B. Eds.; Mat. Res. Soc.: Boston, 1987; p 112.
(42) Francis, A. H.; Kopelman, R. *Topics in Applied Physics, Laser Spectroscopy of Solids*, 2nd ed.; Yen, W. M., Selzer, P. M., Eds.; Springer-Verlag: Berlin, 1986; Vol. 49, p 241.
(43) Li, C. S.; Shi, Z.-Y.; Kopelman, R. *J. Lumin.*, in press.
(44) Harmon, L. A.; Kopelman, R. *J. Phys. Chem.*, in press.

Registry No. P1VN, 25135-12-0; PMMA, 9011-14-7.